Biomaterials 125 (2017) 81–89

Contents lists available at ScienceDirect

Biomaterials

journal homepage: www.elsevier.com/locate/biomaterials

Lipopolyplex potentiates anti-tumor immunity of mRNA-based vaccination

Stefano Persano [a, b, c, 1], Maria L. Guevara [a, d, 1], Zhaoqi Li [a], Junhua Mai [a], Mauro Ferrari [a, e], Pier Paolo Pompa [b], Haifa Shen [a, f, *]

[a] Department of Nanomedicine, Houston Methodist Research Institute, 6670 Bertner Ave, Houston, TX, 77030, USA
[b] Nanobiointeractions & Nanodiagnostics, Istituto Italiano di Tecnologia (IIT), Via Morego, 30, 16163, Genova, Italy
[c] Università del Salento, Via Provinciale Monteroni, 73100, Lecce, Italy
[d] Escuela de Ingenieria y Ciencias, Tecnologico de Monterrey, Monterrey, NL, 64849, Mexico
[e] Department of Medicine, Weill Cornell Medical College, 1330 York Ave, New York, NY, 10065, USA
[f] Department of Cell and Developmental Biology, Weill Cornell Medical College, 1330 York Ave, New York, NY, 10065, USA

ARTICLE INFO

Article history:
Received 24 November 2016
Received in revised form
14 February 2017
Accepted 14 February 2017
Available online 21 February 2017

Keywords:
Cancer
Immunotherapy
Lipopolyplex
mRNA
Vaccine

ABSTRACT

mRNA-based vaccines have the benefit of triggering robust anti-cancer immunity without the potential danger of genome integration from DNA vaccines or the limitation of antigen selection from peptide vaccines. Yet, a conventional mRNA vaccine comprising of condensed mRNA molecules in a positively charged protein core structure is not effectively internalized by the antigen-presenting cells. It cannot offer sufficient protection for mRNA molecules from degradation by plasma and tissue enzymes either. Here, we have developed a lipopolyplex mRNA vaccine that consists of a poly-(β-amino ester) polymer mRNA core encapsulated into a 1,2-dioleoyl-*sn*-glycero-3-ethylphosphocholine/1,2-dioleoyl-*sn*-glycero-3-phosphatidyl-ethanolamine/1,2-distearoyl-*sn*-glycero-3-phosphoethanolamine-*N*-[amino(poly-ethylene glycol)-2000 (EDOPC/DOPE/DSPE-PEG) lipid shell. This core-shell structured mRNA vaccine enters dendritic cells through macropinocytosis. It displayed intrinsic adjuvant activity by potently stimulating interferon-β and interleukin-12 expression in dendritic cells through Toll-like receptor 7/8 signaling. Dendritic cells treated with the mRNA vaccine displayed enhanced antigen presentation capability. Mice bearing lung metastatic B16-OVA tumors expressing the ovalbumin antigen were treated with the lipopolyplex mRNA, and over 90% reduction of tumor nodules was observed. Collectively, this core-shell structure offers a promising platform for mRNA vaccine development.

1. Introduction

Therapeutic vaccine has a huge potential in the treatment of multiple types of life-threatening diseases including cancer and infectious diseases. A key issue to determine success of cancer vaccination is potent induction of anti-tumor responses against the antigen of choice. Both protein peptides and DNA plasmids have traditionally served as antigens for vaccine development [1–3]. Protein peptides are relatively easy to prepare and can be produced in a large scale; however, the choice of antigen peptide is dependent on the patient's unique type of major histocompatibility complex (MHC) proteins, and thus needs to be customized to match with individual patients. On the other hand, DNA vaccines suffer from low potency and run the risk of uncontrolled genomic integration [4]. mRNA has recently emerged as an ideal antigen source for cancer vaccines [5]. mRNA molecules cannot only be tailored to encode multiple antigens, but also serve as an adjuvant by triggering Toll-like receptor (TLR) signaling in the antigen-presenting cells [6–8]. In addition, mRNA-mediated gene transfer can occur in non-dividing cells since nuclear translocation and transcription is not required, while plasmid DNA-mediated gene transfer is mostly effective in dividing cells [4,9].

Multiple approaches have been tried to introduce mRNA into antigen-presenting cells. It has been shown that local injection of naked mRNA could lead to a specific immune response [10–12]. However, this strategy did not lead to high levels of protein

* Corresponding author. Department of Nanomedicine, Houston Methodist Research Institute, 6670 Bertner Ave., Houston, TX, 77030, USA.
E-mail address: hshen@houstonmethodist.org (H. Shen).
[1] These authors contributed equally to the work.

http://dx.doi.org/10.1016/j.biomaterials.2017.02.019
0142-9612/

expression, as naked mRNA molecules are immediately degraded by tissue nucleases [13]. Since the negatively charged mRNA molecules cannot enter antigen-presenting cells directly, mRNA-based vaccine is usually prepared by transfecting mRNA molecules into patient-derived dendritic cells (DCs) by electroporation [14,15]. The DC vaccine is then reintroduced back to the patient for tumor antigen synthesis, processing and presentation. A number of DC vaccines have reached different stages of clinical trials [15–17]. However, this procedure does not allow mass production of off-the-shelf therapeutic vaccines. An alternative approach to prepare the mRNA vaccine is to package mRNA molecules in nanoparticles and directly inoculate them into the body where the vaccine is taken up by the antigen-presenting cells [18,19]. This approach takes advantage of the high phagocytic capacity of antigen-presenting cells. The protamine-condensed mRNA vaccines and RNA lipoplex vaccines consist an important part in this group, and several of them are at different stages of preclinical studies and clinical trials [20,21]. Condensing mRNA into particles not only enables cellular uptake of mRNA vaccine, but also facilitates stimulation of MyD88-dependent TLR-7/8 signaling in the host cells [22]. However, mRNA degradation is a potential concern, as part of the naked mRNA is exposed to the body fluid and is vulnerable to attack by plasma and tissue RNases. In addition, exposure of the mRNA molecules to non-antigen-presenting cells runs the risk of triggering adverse reactions inside the body.

In this study, we have designed a lipopolyplex (LPP) platform to package mRNA molecules into a polymeric polyplex core that is loaded into a phospholipid bilayer shell structure (Fig. 1a). The resulting construct can not only protect mRNA molecules in the polyplex core structure from RNase attack but also be efficiently internalized by DCs where the particle is transported through the vesicular system and mRNA molecules are released to the cytosol for antigen production. We have systematically characterized composition and morphology of the LPP, and studied cellular uptake of LPP/mRNA by DCs and protein synthesis in these cells. By applying ovalbumin (OVA) and tyrosinase-related protein 2 (TRP2) as antigens, we have examined immune responses to these vaccines in cell culture, and evaluated anti-tumor immunity in murine models of melanoma lung metastasis.

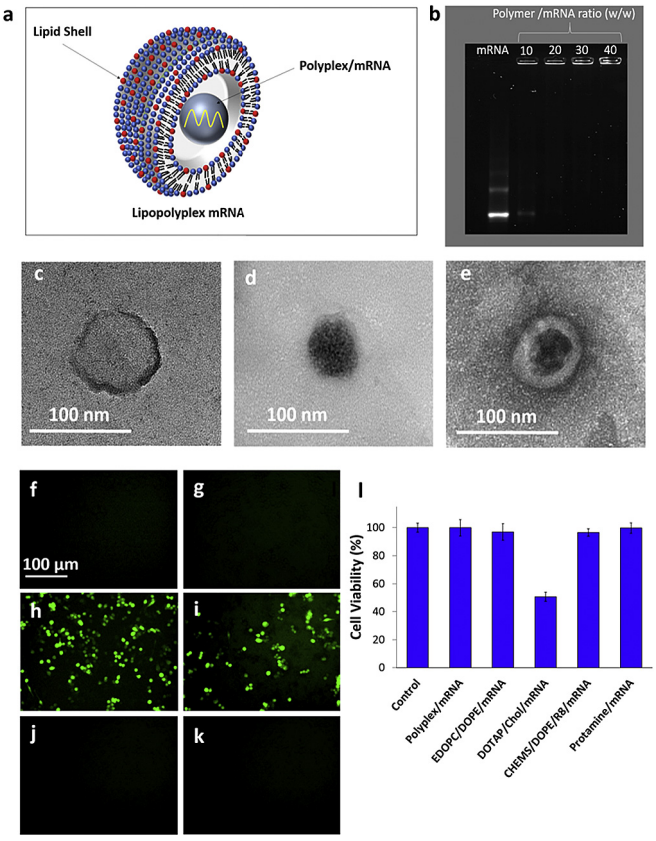

Fig. 1. Structure and characterization of lipopolyplex mRNA vaccine. (**a**) Schematic view of the lipopolyplex mRNA vaccine. The vaccine is composed of a polyplex core assembled through electrostatic interaction between the positively charged PbAE polymer and the negatively charged mRNA molecule. The polyplex is encapsulated into a lipid shell. (**b**) Gel retardation assay on polyplex-mRNA binding. Samples were loaded in the following order: free mRNA, polyplex/mRNA with 10, 20, 30 and 40 (w/w). (**c-e**) TEM images of the empty liposomal shell (c), polyplex/mRNA core (w/w = 20) (d), and lipopolyplex/mRNA core-shell structure (e). (**f-k**) eGFP expression in DC2.4 cells treated with mRNA-packaged particles. DC2.4 cells were treated with (f) PBS control, g) PbAE/eGFP mRNA core, h) EDOPC/DOPE-packaged PbAE/eGFP mRNA, i) DOTAP/Chol-packaged PbAE/eGFP mRNA, j) CHEMS/DOPE/R8-packaged PbAE/eGFP mRNA or k) protamine/eGFP mRNA core, and eGFP expression was detected under a fluorescent microscope 24 h later. **l)** DC2.4 viability upon treatment with the different particles.

2. Materials and methods

2.1. Synthesis of poly-(β-amino ester) polymer (PbAE)

The PbAE (MW ~4 kDa) was synthesized in a two-step reaction procedure as previously described [23]. In the first step, the base polymer was synthesized by mixing 1,4-butanediol diacrylate (Sigma-Aldrich) with 5-amino-1-pentanol (Sigma-Aldrich) at a molar ratio of 1.2:1. The reaction was maintained at 90 °C for 24 h in a glass scintillating vial with a teflon stir bar. The base polymer was dried, and then dissolved in anhydrous dimethyl sulfoxide (DMSO) at a final concentration of 167 mg/mL. In the second step, 480 μL of the base polymer solution was mixed with 320 μL of 0.5 mol/L $(PEO)_4$-bis-amine (Molecular Biosciences, Boulder, CO) in a 1.5-mL Eppendorf tube, and the reaction was allowed for 24 h at room temperature. The polymer mix was first dialyzed against milli-Q water in a dialysis tube (MWCO 3500 Da) to remove the bulk of free reagents, and then mixed with 4× the volume of ethyl ether (Sigma-Aldrich) and vortexed vigorously followed by centrifugation at 4000 rpm for 5 min to further remove unreacted monomers in the supernatant. The purified polymers were vacuum-dried and then dissolved in 25 mM sodium acetate, pH 5.2.

2.2. Preparation of PbAE/mRNA polyplex

PbAE/mRNA polyplex was prepared by mixing one volume of the PbAE polymer with two volumes of mRNA molecules (Trilink Biotechnologies, San Diego, CA). After incubation for 20 min at 20 °C, the polyplex was analyzed for size distribution and zeta potential using a Malvern Zetasizer Nano ZS dynamic light scattering instrument (Malvern Instruments, Worcestershire, UK). The PbAE/mRNA polyplex was also analyzed in a gel retardation assay. Briefly, a polyplex sample containing 250 ng mRNA was loaded into each well and separated by electrophoresis in a 0.7% agarose gel with 1 × TBE buffer (BioRad, Hercules, CA). RNA bands were stained with Gelred nucleic acid gel stain (Biotium, Hayward, CA) and visualized with a GelDoc system (BioRad, Hercules, CA).

2.3. Preparation and characterization of LPP/mRNA vaccines

The lipids 1,2-dioleoyl-*sn*-glycero-3-ethylphosphocholine (EDOPC), 1,2-dioleoyl-*sn*-glycero-3-phosphatidyl-ethanolamine (DOPE), 1,2-distearoyl-*sn*-glycero-3-phosphoethanolamine-*N*-[amino(polyethylene glycol)-2000 (DSPE-PEG-2000), cholesteryl

hemisuccinate (CHEMS) and 1,2-dioleoyl-3-trimethylammonium-propane (DOTAP) were purchased from Avanti Polar Lipids (Birmingham, Alabama, USA). Cholesterol was obtained from Sigma-Aldrich (Saint Louis, MO, USA). The reagents were dissolved in chloroform at a final concentration of 20 mg/mL and applied to prepare thin lipid films by rotary evaporation in a Buchi Rotavapor (Oldham, UK) under partial vacuum. The thin lipid film was composed of 49% EDOPC, 49% DOPE and 2% DSPE-PEG. The lipid film was rehydrated with a solution containing PbAE/mRNA polyplex to prepare the lipopolyplex mRNA vaccine. Size distribution and zeta potential of the LPP/mRNA vaccine were measured with DLS and transmission electronic microscopy (TEM). The same procedure was applied to prepare CHEMS/DOPE/octaarginine (CHEMS/DOPE/R8) and DOTAP/Cholesterol/DSPE-PEG-2000 (DOTAP/Chol/DSPE-PEG-2000) lipopolyplexes. To prepare protamine/mRNA polyplex, protamine sulfate (grade X, Sigma Aldrich) was mixed with mRNA at weight ratio of 2:1 in 10 mM Tris-HCL buffer, followed by a 30-min incubation at room temperature.

2.4. Cellular uptake of LPP/mRNA vaccine in vitro

Immortalized DC2.4 (a murine bone marrow derived dendritic cell line) cells were applied to test protein expression from the LPP/mRNA vaccine. Briefly, cells were seeded in a 24-well plate at a seeding density of 1.5×10^5 cells/well, and cell culture was maintained in 1 mL RPMI-1640 complete medium (supplemented with 10% fetal bovine serum [FBS, Atlas Biological, Fort Collins, CO], 1% penicillin/streptomycin [10,000 units penicillin and 10 mg streptomycin, Sigma-Aldrich, Saint Louis, MO] and 0.1% β-mercaptoethanol [Sigma-Aldrich]). Cells were incubated with LPP packaged with 0.5 μg eGFP mRNA (LPP/eGFP mRNA) for 24 h, and eGFP expression was visualized using an Eclipse TE2000-S fluorescent microscope (Nikon Corporation, Tokyo, Japan). Flow cytometry was performed to measure percentage of GFP-positive cells using a BD Accuri C6 flow cytometer (Becton Dickinson, BD, Franklin Lakes, NJ, USA). The same procedure was also applied to determine eGFP expression in human MDA-MB-231 breast cancer cells (ATCC; Manassas, VA) and murine mDMEC skin endothelial cells after they were incubated with LPP/eGFP mRNA, respectively.

To determine route of cellular internalization of the LPP/mRNA vaccine, DC2.4 cells were seeded at a density of 1.5×10^5 cells/well in a 24-well plate and incubated for 24 h at 37 °C. They were then treated with FAM-labeled mRNA packaged in LPP (LPP/FAM-mRNA) and one of the following small molecule inhibitors: amiloride (0.2 mM), chloroquine (100 mM), genistein (50 μM), chlorpromazine (15 μM), or pimozide (10 μM). Cells were allowed to grow for 4 h before they were washed with ice-cold PBS and applied to determine particle uptake under the fluorescent microscope.

2.5. Cytotoxicity from LPP/mRNA in vitro

To test potential cytotoxicity from LPP/mRNA vaccine, DC2.4, MDA-MB-231 and Endothelial cells were seeded in a 96-well plate at a seeding density of 3×10^4 cells/well, and treated with LPP/0.1 μg mRNA. Cell viability was measured 24 h later with a tetrazolium-based CellTiter 96® Aqueous One Solution Cell Proliferation (MTS) assay (Promega, Madison, WI) following the manufacturer's instruction.

2.6. Preparation of bone marrow-derived dendritic cells (BMDCs)

BMDCs were prepared from C57BL/6 mice as previously described [24]. Briefly, bone marrow cells from the femur and tibia were flushed out with 2% FBS-containing phosphate buffer saline (PBS) using a syringe. Cells were centrifuged at 500×*g* for 4 min, treated with ACK lysis buffer (Lonza Inc) to remove red blood cells, and resuspended in RPMI-1640 culture medium supplemented with 10% FBS, 0.5% β-mercaptoethanol, 1% penicillin/streptomycin, 20 ng/mL granulocyte-macrophage colony-stimulating factor (GM-CSF), and 20 ng/mL interleukin-4 (IL-4). They were seeded into 6-well plates at a seeding density of 1×10^6 cells/mL, and growth medium was changed every other day. The non-adherent dendritic cells were harvested on day 5.

2.7. Measurement of pro-inflammatory cytokines

BMDCs were seeded at a density of 3×10^5 cells/well in a 24-well plate, and treated with LPP/0.5 μg OVA mRNA. Disassembled components of the LPP/mRNA vaccine (the liposome shell and the polyplex core) served as negative controls. After 24 h of incubation, supernatants were collected, and IL-6, TNF-α, IFN-β and IL-12 concentrations were measured with an ELISA kit for cytokine measurement (eBioscience, San Diego, CA). To measure serum IFN-β level in vaccinated mice, C57BL/6 mice were vaccinated s.c. with 2.5 μg LPP/OVA-mRNA and serum was collected 3, 6 and 24 h later. Serum IFN-β level was determined with the ELISA kit (eBioscience, San Diego, CA).

2.8. TLR7/8 inhibition

DC2.4 cells were seeded in a 24-well plate at a density of 1.5×10^5 cells/1 mL RPMI-1640 complete medium, and incubated for 24 h at 37 °C. Cells were then treated with the TLR7/8 inhibitor ODN 2087 (Militenly Biotec, San Diego, CA, USA) at a final concentration of 2.5 μM for 1 h at 37 °C. Subsequently, LPP/0.5 μg OVA mRNA was added into the culture, and cell growth was maintained for another 24 h before cell culture medium was collected for cytokine analysis. Dendritic cells without TLR inhibitor treatment served as the positive control, and cells without LPP/OVA mRNA treatment were used as the negative control.

2.9. Evaluation of dendritic cell maturation

DC2.4 cells were seeded in 24-well plates at a density of 1.5×10^5 cells/well supplied with 1 mL RPMI complete medium. They were treated with LPP/0.5 μg mRNA and incubated at 37 °C for 24 h. Cells were then washed with PBS, stained with antibodies specific for CD11c, CD40, CD86 and MHC II (BD Bioscience), and applied for flow cytometry analysis with a BD Accuri C6 flow cytometer (Becton Dickinson, BD, Franklin Lakes, NJ, USA).

2.10. MHC I and II–restricted antigen presentation assays

To measure antigen presentation, BMDCs treated with LPP/OVA mRNA were stained for 10 min at room temperature with a pentamer that recognize the OVA257-264 - H-2Kb complex (H-2Kb/SIINFEKL, BD Bioscience, San Jose, CA). Cells were then stained for 30 min with an anti-CD11c antibody (BD Bioscience) and analyzed using a BD Accuri C6 flow cytometer (BD Bioscience, San Jose, CA).

To determine T cell activation, BMDC and DC2.4 cells were treated with LPP/0.5 μg OVA mRNA for 24 h. Cells were washed with PBS and co-cultured either with B3Z OVA-specific CD8 T cells or DOBW OVA-specific CD4 T cells at a DC/T cell ratio of 1:1. ELISA was performed to measure IL-2 secretion by the activated T cells. All samples were measured in triplicate.

2.11. In vitro killing of B16-OVA melanoma cells by cytotoxic T cell

DC2.4 were seeded at a density of 1.5×10^5 cells/well in a 24-well plate. After overnight incubation, cells were treated with

LPP/0.5 μg OVA mRNA for 24 h at 37 °C. These DC2.4 cells were subsequently co-cultured with B3Z T cells at a DC2.4/T cell ratio of 1:2. After 24 h of incubation, the activated T cells were applied to co-culture with B16 melanoma cells at T cell/tumor cell ratio of 5:1 for 4, 8 or 24 h at 37 °C. Tumor cell viability was then determined using a MTS formazan viability assay (Promega, Madison, WI) as described above. Tumor cells treated with non-activated T cells or with T cells activated with a HER2 breast cancer antigen peptide served as negative controls. All samples were measured in triplicate.

2.12. Bioluminescence imaging in live mice

BALB/c mice were administered subcutaneously with 10 μg of luciferase mRNA loaded into LPP (LPP/Luc mRNA). Mice were injected intraperitoneally with 30 μg RediJect D-luciferin Ultra (Perkin-Elmer) 24 or 48 h later, and bioluminescence was measured in a Xenogen IVIS-200 imaging system.

2.13. Efficacy test in murine model of lung metastatic melanoma

Eight-week-old male and female C57BL/6 mice were inoculated with 2.5×10^5 B16-OVA melanoma tumor cells by tail vein injection to establish lung metastatic tumors following a previously described protocol [25]. Three days after tumor inoculation, mice were subcutaneously vaccinated with LPP/OVA mRNA (1 μg). Vaccination was boosted at days 7 and 10 with two more inoculations. Mice were euthanized on day 18, and lungs were harvested and fixed with 4% paraformaldehyde. Number of lung metastatic tumor nodules was counted under a dissecting microscope.

2.14. In vivo T cell activation analysis

To determine T cell activation status, C57BL/6 mice were immunized s.c with 2.5 μg LPP/OVA mRNA. To determine T cell activation by surface marker, mice were euthanized 24 h later, and spleen and lymph nodes were collected, processed and stained with an anti-murine CD3, CD4, CD8 or CD69 antibody (Ebioscience) for 30 min at 4 °C, and then analyzed by flow cytometry using BD Accuri C6 flow cytometer (BD Bioscience, San Jose, CA). To measure T cell activation by IFN-γ secretion, C57BL/6 were immunized s.c with LPP/OVA mRNA or LPP/TRP2 mRNA at days 1, 4 and 7. One week after the last immunization, spleen and lymph nodes and PBMCs were collected and processed for single cell analysis. Cells were re-stimulated with OT-I ($OVA_{257-264}$), OT-II ($OVA_{323-339}$), or PMA-Ionomycin for 48 h at 37 °C. IFN-γ secretion was analyzed by ELISA (eBioscience).

2.15. Statistical analysis

Two-tailed Student *t*-test was applied for comparison between experimental groups. $P < 0.05$ was considered statistically significant.

3. Results

3.1. Lipopolyplex-based mRNA vaccine is optimal for dendritic cell uptake and protein expression

We designed a novel platform for mRNA-based vaccine that consisted of a PbAE/mRNA polyplex core structure packaged into a lipid bilayer envelope (Fig. 1a). Agarose gel electrophoresis was applied to examine mRNA binding capacity to the cationic PbAE polymer, and it was determined that mRNA was fully encapsulated into PbAE when PbAE/mRNA ratio (w/w) was 20 or beyond (Fig. 1b). Consequently, a PbAE/mRNA ratio of 20 was chosen to prepare LPP mRNA vaccines in the rest of the study. TEM analysis detected a 50 nm PbAE/mRNA polyplex core (Fig. 1d) surrounded by an EDOPC/DOPE/DSPE-PEG-2000 lipid shell (Fig. 1c and e).

Lipid shell for the LPP/mRNA vaccine was compared among EDOPC/DOPE/DSPE-PEG-2000, DOTAP/Chol/DSPE-PEG-2000 and CHEMS/DOPE/R8. DOTAP/Chol/DSPE-PEG-2000 forms a cationic lipid shell, and CHEMS/DOPE/R8 is a lipid shell with an active targeting moiety; both have previously been applied for RNA delivery [26,27]. DC2.4 served as the antigen presenting cells and mRNA molecules encoding the eGFP protein was applied to prepare the polyplex core. Cells incubated with the PbAE/mRNA core did not express a detectable level of eGFP (Fig. 1g). While cells treated with EDOPC/DOPE/DSPE-PEG-2000 and DOTAP/Chol/DSPE-PEG-2000-packaged particles expressed bright eGFP proteins, those incubated with CHEMS/DOPE/R8-packaged polyplex did not have a detectable level of eGFP (Fig. 1h–j). Interestingly, cells treated with protamine/eGFP did not have a high level of eGFP expression either (Fig. 1k), in line with a previous report with a similar delivery platform [28]. In addition, we detected a high level of cytotoxicity from the DOTAP/Chol/DSPE-PEG-2000 formulation (Fig. 1). Consequently, EDOPC/DOPE/DSPE-PEG-2000 was selected for LPP/mRNA vaccine preparation in all follow-up studies.

3.2. LPP/mRNA vaccine enters dendritic cells through macropinocytosis

Uptake of the LPP/mRNA vaccine particles by different cell types was investigated. An equal amount of EDOPC/DOPE/DSPE-PEG-2000 particles packaged with PbAE/eGFP mRNA was added into culture of DC 2.4 cells, MDA-MB-231 human breast cancer cells, the mDMEC murine endothelial cells, B3Z hybridoma T cells, murine B lymphoma cells, or the Raw246.7 murine macrophage cells, and cells expressing eGFP were detected 24 h later. In line with the notion that DCs are the most effective antigen-presentation cells with a high phagocytic potential [29], all DC2.4 cells had internalized the vaccine particles and expressed the green fluorescent protein; in comparison, about half number of MDA-MB-231 cells and macrophages were GFP-positive, and only a small fraction of the B, T, and endothelial cells synthesized GFP (Fig. 2a). To ensure protein expression by the LPP/mRNA *in vivo*, we treated mice with LPP packaged with luciferase mRNA (LPP/Luc). Strong bioluminescent signal was detected 48 h later in the abdominal cavity where the mesenteric lymph nodes locate (Fig. 2b).

We examined mechanism of cellular uptake by treating DC2.4 cells with inhibitors of endocytosis, macropinocytosis and

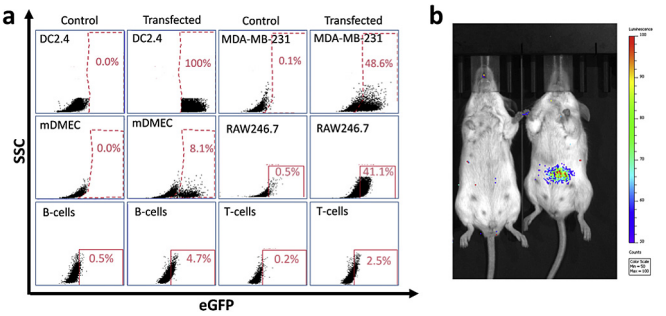

Fig. 2. Preferential uptake of the lipopolyplex mRNA vaccine by dendritic cells. (a) Flow cytometry analysis on GFP-positive cells after DC2.4, MDA-MB-231 and mDMEC cells were incubated with lipopolyplex/eGFP mRNA for 24 h. (b) Bioluminescent image to detect luciferase expression in mice 48 h after s.c. injection of LPP/Luc. Left: control mouse; right: LPP/Luc-treated mouse.

phagocytosis. Treatment with amiloride, an inhibitor of macropinocytosis [30], and cytochalasin D, a potent inhibitor of actin polymerization which is a macropinocytosis-dependent process, reduced cellular uptake of the EDOPC/DOPE/DSPE-PEG-2000-packaged FAM fluorescent dye-labeled mRNA (LPP/FAM-mRNA) by 70% and 80%, respectively. In comparison, cellular uptake of the particles was not significantly affected by the caveolin-mediated endocytosis inhibitor genistein, the clathrin-mediated endocytosis inhibitor chlorpromazine, the phagocytosis inhibitor pimozide, or the microtubule polymerization inhibitor nocodazole (Fig. 3a–h). The result suggests that macropinocytosis was the major route of cell entry for the LPP mRNA vaccine. Chloroquine, a reagent that prevents endosome acidification and maturation, did not affect mRNA accumulation either (Fig. 3d). Time-dependent monitoring of cells treated with LPP packaged with FAM-mRNA (LPP/FAM-mRNA) showed a delayed increase in fluorescent intensity, with a high intensity level reached 120 min after incubation (Fig. 3j), indicating the mRNA molecules exited endosomes and entered the cytosol successfully.

3.3. LPP mRNA vaccine promotes DC maturation

Murine tumor models with an overexpressed ovalbumin (OVA) have been widely applied to test the effectiveness of cancer vaccines [31–33]. We applied OVA mRNA to assemble the therapeutic mRNA vaccine (LPP/OVA), and examined anti-tumor immunity *in vitro* and *in vivo*. In an *in vitro* setting, bone marrow-derived DCs (BMDCs) were co-incubated either with LPP/OVA or controls, and cytokine levels in the cell growth media were measured. Interestingly, both the polyplex/OVA core and LPP/OVA, together with protamine/OVA, could trigger significant TNF-α expression (Fig. 4a). It has been previously reported that TNF-α-dependent DC maturation is critical for activating the adaptive immune responses to virus infection [34] and for anti-tumor immunity [35]. However, neither polyplex/OVA nor protamine/OVA was as potent as LPP/OVA in stimulating IFN-β and IL-12 expression (Fig. 4a). We have previously shown that the type I interferon IFN-β promotes DC maturation, antigen processing and presentation, and stimulation of T cell clonal expansion [24]. Likewise, IL-12 is one of the Th1 cytokines [36], and DCs that produce IL-12 promote type I $CD8^+$ T cell immunity [37,38]. In a separate study, we treated DCs with LPP/OVA mRNA (0.5 and 1 μg) or LPP/OVA protein (10 and 100 μg), and compared IFN-β and IL-12 secretion. At the given doses, the mRNA-based vaccines induced higher levels of cytokine production (Fig. 4c). The results indicate that both the polyplex/mRNA core and the lipid shell are needed in order to maximize the adjuvant effect from the vaccine. LPP/mRNA-mediated adjuvant effect was mediated through activation of the TLR-7/8 signaling, in line with the protamine-condensed mRNA particles [22,39], as treatment with the short single-stranded oligodeoxynucleotide TLR7/8 inhibitor ODN2087 completely suppressed LPP/OVA-stimulated IL-12 and IFN-β expression (Fig. 4b).

DC maturation markers were examined in the LPP/OVA-treated DC2.4 cells. The post-treatment cells had dramatically increased level of MHC II expression (Fig. 4d). It has been reported that DCs express a higher level of MHC II loaded with peptides derived from antigens at the plasma membrane upon activation [40]. In addition, levels of the other DC maturation markers, CD40 and CD86, were also higher in the treated cells (Fig. 4d).

3.4. LPP mRNA vaccine stimulates antigen presentation

Antigen processing and presentation were analyzed in BMDCS treated with LPP/OVA. Flow cytometry detected $CD11c^+$ DCs that also displayed MHCI-OVA epitope on cell surface (Fig. 5a). When the post-treatment cells were co-incubated with OVA-specific $CD4^+$ or $CD8^+$ T cells, we detected significant increases in IL-2 secretion by the antigen-specific T cells (Fig. 5b), indicating the DCs had successfully processed and presented OVA epitopes that could be recognized by the T cells. These results demonstrate that BMDCs can properly translate the mRNA antigen, and process and present the antigen epitopes. In a separate study, we observed similar effects with the post-treatment DC2.4 cells (Fig. 5c). Furthermore, we compared the ability of DC2.4 cells pulsed with LPP/OVA mRNA or LPP/OVA protein to activate naïve T cells *in vitro*, and found those primed with LPP/OVA mRNA triggered a higher level of IL-2 secretion by T cells (Fig. 5d). The results demonstrate that the mRNA-based vaccine has a higher immunogenic potential comparing to the protein-based vaccine, thanks to its ability to activate innate immunity and enhance T cell priming.

3.5. LPP mRNA vaccine has a potent anti-tumor activity

In vivo LPP/OVA mRNA vaccination recapitulated the DC maturation and T cell stimulation phenotypes. A significantly higher level of serum IFN-β was detected 6 h after vaccination (Fig. 6a), and stimulation of $CD4^+$ and $CD8^+$ T cells in the lymph nodes and spleen was determined based on positive staining of the CD69 maturation marker (Fig. 6b). Cells isolated from the spleens or lymph nodes in mice after 3 treatments with LPP/OVA mRNA vaccine had a more robust IFN-γ production by the $CD4^+$ and $CD8^+$ T cells upon rechallenge with the OT-I and OT-II peptides than those from mice treated with a liposomal OVA protein vaccine (Fig. 6c). To test tumor cell killing *in vitro*, we co-cultured the activated OVA-specific T cells with B16-OVA melanoma cells at an effector T cell/tumor cell ratio of 5:1, and examined time-dependent tumor cell killing. A significant decrease in B16-OVA tumor cell viability was observed as early as 4 h after co-incubation, and most tumor cells were dead by the 24-h time

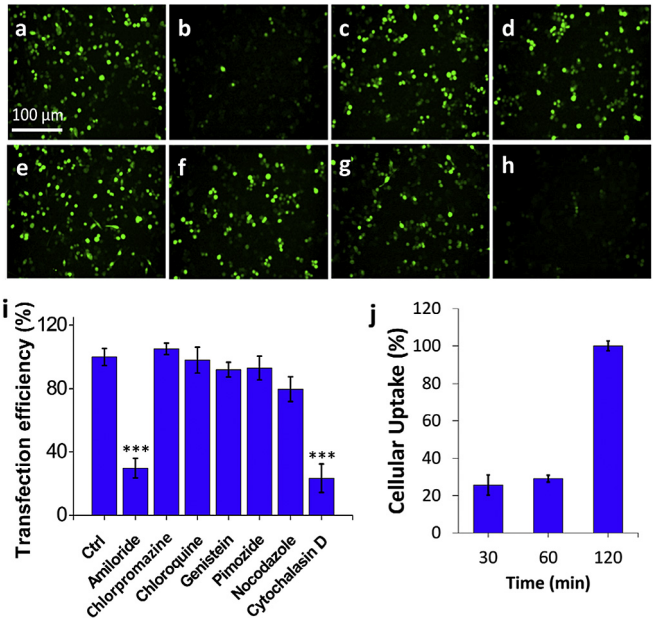

Fig. 3. Mechanism of cell entry. (**a**–**h**) Images of DC2.4 cells treated with LPP/0.5 μg FAM-labeled eGFP mRNA for 4 h in presence of (a) mock control, (b) amiloride, (c) chlorpromazine, (d) chloroquine, (e) genistein, (f) pimozide, (g) nocodazole, and (h) cytochalasin D. (**i**) Image J analysis on FAM-positive cells. (**j**) Time-dependent uptake of LPP/FAM-labeled eGFP mRNA by DC2.4 cells. Error bars represent the mean ± standard deviation of triplicate experiments.

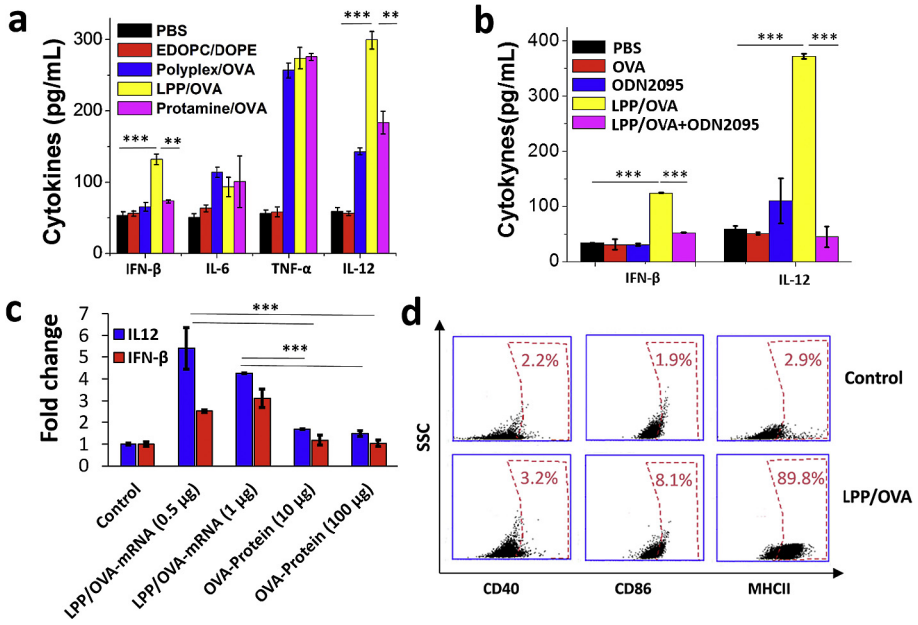

Fig. 4. DC stimulation by the LPP/mRNA vaccine. a) Cytokine secretion in BMDCs treated with LPP/OVA (EDOPC/DOPE/DSPE-PEG packaged with OVA mRNA) and controls. **b**) Inhibition of IL-12 and IFN-β expression by the TLR7/8 inhibitor ODN2087. **c**) Comparison between LPP/OVA mRNA and LPP/OVA protein on DC stimulation. **d**) Flow cytometry analysis on DC maturation markers. Error bar represents the mean ± standard deviation of triplicate experiments.

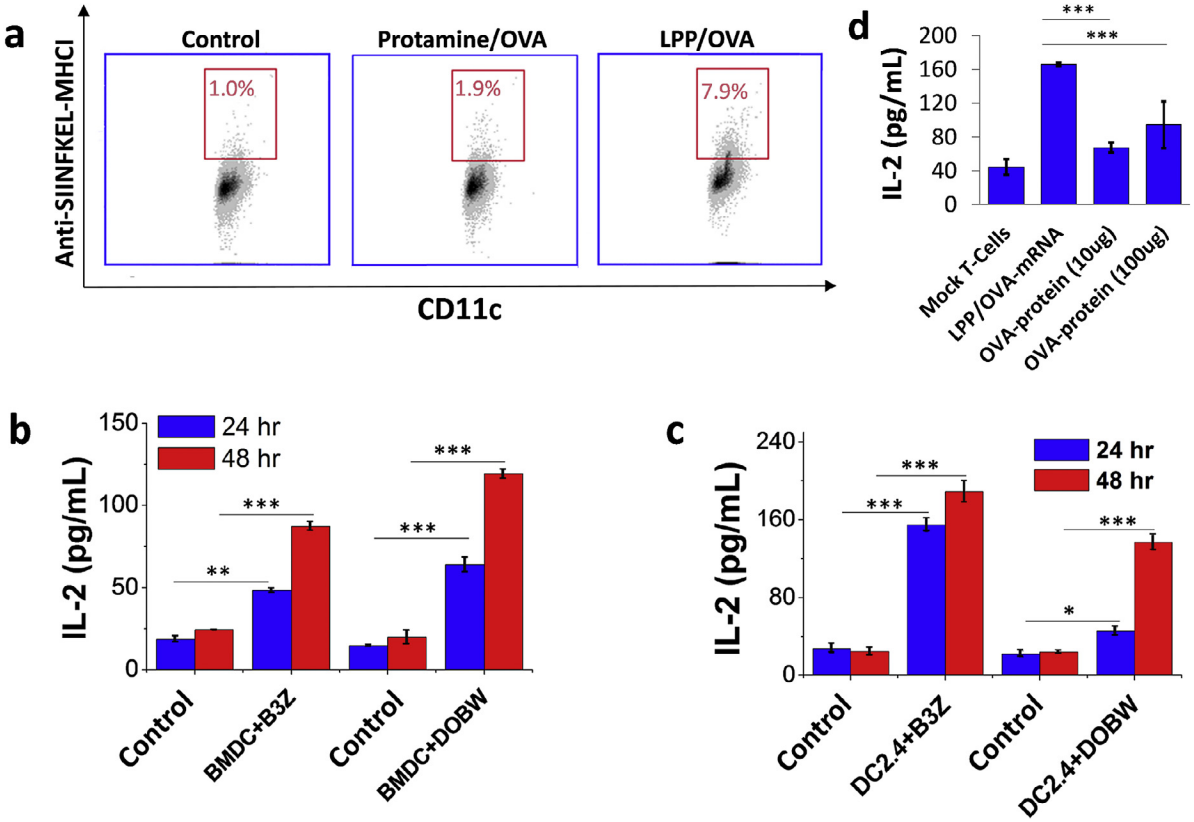

Fig. 5. Stimulation of DC antigen cross-presentation by the LPP/mRNA vaccine. a) Flow cytometry analysis on H-2k^{b}-OVA$_{257-264}$ presentation. **b**) Time-dependent IL-2 secretion by OVA-specific CD4^{+} and CD8^{+} T cells after co-incubation with post-treated BMDCs. B3Z: OVA-specific CD8^{+} T cell; DOBW: OVA-specific CD4^{+} T cell. **c**) Time-dependent IL-2 secretion by OVA-specific CD4^{+} and CD8^{+} T cells after co-incubation with post-treated DC2.4 cells. **d**) Comparison of IL-2 secretion by OVA-specific CD8^{+} T cells after co-incubation with DC2.4 cells pretreated with LPP/OVA mRNA or LPP/OVA protein.

point (Fig. 6d). In comparison, tumor cells treated with naïve T cells or T cells primed with liposomal OVA protein did not show a significant cell death. To confirm antigen-specific tumor cell killing, we co-incubated B16-OVA cells with T cells specific for the HER2 breast cancer antigen, but not OVA, and no cell death was observed (data not shown).

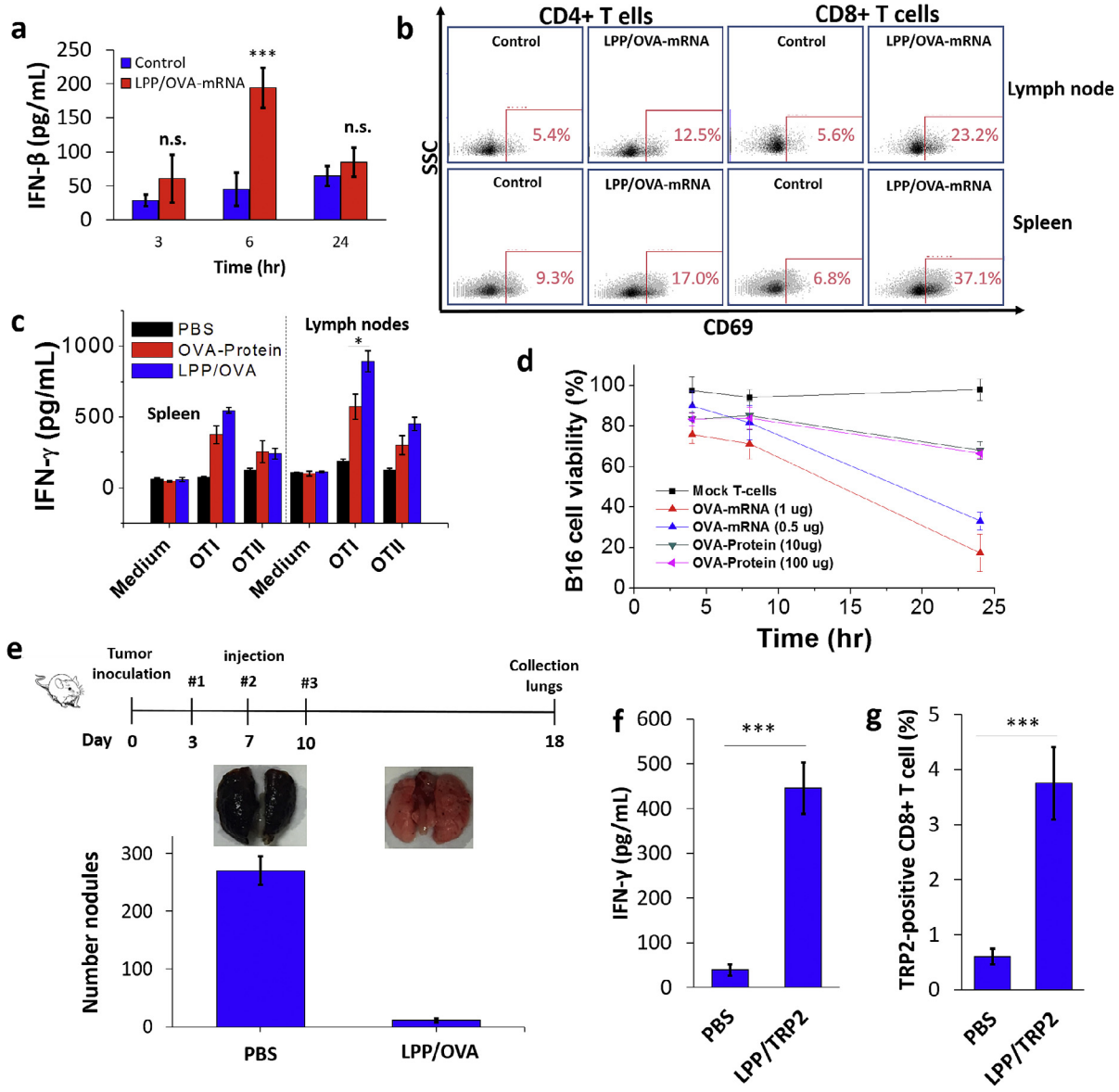

Fig. 6. Anti-tumor activity from LPP/mRNA *in vitro* and *in vivo*. **a**) Serum IFN-β levels 3, 6, and 24 h after s.c. LPP/OVA mRNA vaccination. **b**) Flow cytometry analysis on T cell activation in LPP/OVA mRNA vaccinated mice. **c**) IFN-γ production by splenocytes and lymph node cells from LPP/OVA mRNA vaccinated miceupon stimulation with OT-I and OT-II. **d**) Time-dependent killing of B16-OVA melanoma cells in culture after co-incubation with antigen-specific T cells. **e**) Inhibition of B16-OVA melanoma lung metastasis by LPP/OVA mRNA. Treatment schedule (top panel) and representative images of the lungs from post-treatment mice (middle panel) are shown, and average number of tumor nodules in the lung is summarized (bottom panel). Data are presented as mean ± SEM. There were 5 mice in each group. **f**) IFN-γ production by PBMCs from mice vaccinated with LPP/TRP2 mRNA. **g**) Percentage of TRP2-specific $CD8^+$ T cells in PBMCs from vaccinated mice.

Anti-tumor activity was further evaluated in a B16-OVA melanoma lung metastasis model. Mice were treated with subcutaneous injection of LPP/OVA three times, and euthanized 8 days after the last treatment to examine tumor growth in the lung. Mice in the PBS control group developed extensive pulmonary metastases; in comparison, those treated with the LPP/OVA mRNA showed a 96% decrease in number of tumor nodules in the lung (Fig. 6e), demonstrating the power of the LPP mRNA vaccine in treating metastatic tumors.

In a separate study, we treated C57BL6 mice bearing B16 melanoma with another mRNA vaccine targeting TRP2 (LPP/TRP2 mRNA). We detected a significant level of IFN-γ expression by PBMCs in the vaccinated mice (Fig. 6f). About 4% total PBMCs were TRP2-specific $CD8^+$ T cells (Fig. 6g). These results demonstrate that the LPP/mRNA platform is not restricted to one mRNA, indicting its potential for broad applications in the fight against cancers.

4. Discussion

Tumor-associated neoantigens are constantly being identified as a result of the massive cancer genome sequencing effort and technology advance in predicting immunogenic tumor mutations [41–43]. This resource has provided us with an unprecedented opportunity to develop immunotherapies based on the unique genetic features of the cancer cells, thus sparring the body from unnecessary attack from the standard-of-care chemotherapy drugs. The mRNA-based vaccine has the flexibility to include multiple neoantigens within the same construct, and the choice of antigen peptide can be tailored based on the unique mutation spectrum of

the individual patient, making precision medicine possible. Yet, development of the enabling technology for cancer vaccine has lagged. The lipopolyplex mRNA vaccine platform described in this study represents an important advance in this direction.

Our analysis has revealed multiple advantages from the mRNA core-lipid shell structured LPP/mRNA vaccine over the conventional compressed mRNA core vaccines. Encapsulating the mRNA core into the lipid shell not only protects mRNA from degradation, but also improves DC uptake of the vaccine particles (Fig. 1). In addition, the lipid shell structure prohibits the mRNA core from interacting with non-antigen-presenting cells, thus limiting potential side effects. Furthermore, the LPP/mRNA vaccine is more potent than the naked mRNA core vaccines in stimulating expression of IFN-β and IL-12 (Fig. 4), cytokines that play an important role in mediating anti-tumor immunity through promoting DC maturation. Moreover, LPP/mRNA is very potent in mediating tumor cell killing. On top of these advantages, a core-shell structure also provides the option to encapsulate soluble adjuvants or other stimulatory molecules in the lipid shell whenever there is a need to further enhance activity of the antigen-presenting cells. All these properties highlight the high potential of this novel technology platform in the development of new immunotherapeutic agents in the era of precision medicine.

Financial support

This work was partially supported by National Institutes of Health grants 1R01CA193880-01A1 (HS) and U54CA210181 (MF), U.S. Department of Defense grant W81XWH-12-1-0414 (MF), the Ernest Cockrell Jr. Distinguished Endowed Chair fund (MF), the Italian Flagship Project NanoMax (SP and PPP) and Consejo Nacional de Ciencia y Tecnologia, CONACyT from Mexico (MLG).

Disclosure of conflicts

The authors declare no competing financial interests.

References

[1] I. Melero, G. Gaudernack, W. Gerritsen, C. Huber, G. Parmiani, S. Scholl, et al., Therapeutic vaccines for cancer: an overview of clinical trials, Nat. Rev. Clin. Oncol. 11 (9) (2014) 509–524.
[2] D.J. Schwartzentruber, D.H. Lawson, J.M. Richards, R.M. Conry, D.M. Miller, J. Treisman, et al., gp100 peptide vaccine and interleukin-2 in patients with advanced melanoma, N. Engl. J. Med. 364 (22) (2011) 2119–2127.
[3] P.W. Kantoff, C.S. Higano, N.D. Shore, E.R. Berger, E.J. Small, D.F. Penson, et al., Sipuleucel-T immunotherapy for castration-resistant prostate cancer, N. Engl. J. Med. 363 (5) (2010) 411–422.
[4] M. McNamara, S. Nair, E. Holl, RNA-based vaccines in cancer immunotherapy, J. Immunol. Res. 2015 (2015) 794528.
[5] B.A. Sullenger, S. Nair, From the RNA world to the clinic, Science 352 (6292) (2016) 1417–1420.
[6] F. Heil, H. Hemmi, H. Hochrein, F. Ampenberger, C. Kirschning, S. Akira, et al., Species-specific recognition of single-stranded RNA via toll-like receptor 7 and 8, Science 303 (5663) (2004) 1526–1529.
[7] S.S. Diebold, T. Kaisho, H. Hemmi, S. Akira, C. Reis e Sousa, Innate antiviral responses by means of TLR7-mediated recognition of single-stranded RNA, Science 303 (5663) (2004) 1529–1531.
[8] J. Devoldere, H. Dewitte, S.C. De Smedt, K. Remaut, Evading innate immunity in nonviral mRNA delivery: don't shoot the messenger, Drug Discov. Today 21 (1) (2016) 11–25.
[9] K.J. Kallen, A. Thess, A development that may evolve into a revolution in medicine: mRNA as the basis for novel, nucleotide-based vaccines and drugs, Ther. Adv. Vaccines 2 (1) (2014) 10–31. PMCID: 3991152.
[10] B. Weide, J.P. Carralot, A. Reese, B. Scheel, T.K. Eigentler, I. Hoerr, et al., Results of the first phase I/II clinical vaccination trial with direct injection of mRNA, J. Immunother. 31 (2) (2008) 180–188.
[11] S. Kreiter, A. Selmi, M. Diken, M. Koslowski, C.M. Britten, C. Huber, et al., Intranodal vaccination with naked antigen-encoding RNA elicits potent prophylactic and therapeutic antitumoral immunity, Cancer Res. 70 (22) (2010) 9031–9040.
[12] S. Van Lint, C. Goyvaerts, S. Maenhout, L. Goethals, A. Disy, D. Benteyn, et al., Preclinical evaluation of TriMix and antigen mRNA-based antitumor therapy, Cancer Res. 72 (7) (2012) 1661–1671.
[13] J. Probst, S. Brechtel, B. Scheel, I. Hoerr, G. Jung, H.G. Rammensee, et al., Characterization of the ribonuclease activity on the skin surface, Genet. Vaccines Ther. 4 (2006) 4. PMCID: 1524753.
[14] V.F. Van Tendeloo, P. Ponsaerts, F. Lardon, G. Nijs, M. Lenjou, C. Van Broeckhoven, et al., Highly efficient gene delivery by mRNA electroporation in human hematopoietic cells: superiority to lipofection and passive pulsing of mRNA and to electroporation of plasmid cDNA for tumor antigen loading of dendritic cells, Blood 98 (1) (2001) 49–56.
[15] D. Benteyn, C. Heirman, A. Bonehill, K. Thielemans, K. Breckpot, mRNA-based dendritic cell vaccines, Expert Rev. Vaccines 14 (2) (2015) 161–176.
[16] S. Wilgenhof, A.M. Van Nuffel, D. Benteyn, J. Corthals, C. Aerts, C. Heirman, et al., A phase IB study on intravenous synthetic mRNA electroporated dendritic cell immunotherapy in pretreated advanced melanoma patients, Ann. Oncol. 24 (10) (2013) 2686–2693.
[17] S. Anguille, E.L. Smits, E. Lion, V.F. van Tendeloo, Z.N. Berneman, Clinical use of dendritic cells for cancer therapy, Lancet Oncol. 15 (7) (2014) e257–67.
[18] A. De Beuckelaer, C. Pollard, S. Van Lint, K. Roose, L. Van Hoecke, T. Naessens, et al., Type I interferons interfere with the capacity of mRNA lipoplex vaccines to elicit cytolytic T cell responses, Mol. Ther. 24 (11) (2016) 2012–2020. PMCID: 5154477.
[19] K. Broos, K. Van der Jeught, J. Puttemans, C. Goyvaerts, C. Heirman, H. Dewitte, et al., Particle-mediated intravenous delivery of antigen mRNA results in strong antigen-specific t-cell responses despite the induction of type I interferon, Mol. Ther. Nucleic acids 5 (2016) e326.
[20] B. Weide, S. Pascolo, B. Scheel, E. Derhovanessian, A. Pflugfelder, T.K. Eigentler, et al., Direct injection of protamine-protected mRNA: results of a phase 1/2 vaccination trial in metastatic melanoma patients, J. Immunother. 32 (5) (2009) 498–507.
[21] L.M. Kranz, M. Diken, H. Haas, S. Kreiter, C. Loquai, K.C. Reuter, et al., Systemic RNA delivery to dendritic cells exploits antiviral defence for cancer immunotherapy, Nature 534 (7607) (2016) 396–401.
[22] B. Scheel, R. Teufel, J. Probst, J.P. Carralot, J. Geginat, M. Radsak, et al., Toll-like receptor-dependent activation of several human blood cell types by protamine-condensed mRNA, Eur. J. Immunol. 35 (5) (2005) 1557–1566.
[23] C.D. Kamat, R.B. Shmueli, N. Connis, C.M. Rudin, J.J. Green, C.L. Hann, Poly(-beta-amino ester) nanoparticle delivery of TP53 has activity against small cell lung cancer in vitro and in vivo, Mol. cancer Ther. 12 (4) (2013) 405–415.
[24] X. Xia, J. Mai, R. Xu, J.E. Perez, M.L. Guevara, Q. Shen, et al., Porous silicon microparticle potentiates anti-tumor immunity by enhancing cross-presentation and inducing type I interferon response, Cell Rep. 11 (2015) 957–966.
[25] W.W. Overwijk, N.P. Restifo, in: John E. Coligan, et al. (Eds.), B16 as a Mouse Model for Human Melanoma. Current Protocols in Immunology, 2001. Chapter 20:Unit 20.1.
[26] Y. Wang, H.-H. Su, Y. Yang, Y. Hu, L. Zhang, P. Blancafort, et al., Systemic delivery of modified mRNA encoding herpes simplex virus 1 thymidine kinase for targeted cancer gene therapy, Mol. Ther. J. Am. Soc. Gene Ther. 21 (2) (2013) 358–367.
[27] Y. Hayashi, H. Hatakeyama, K. Kajimoto, M. Hyodo, H. Akita, H. Harashima, Multifunctional envelope-type Nano device: evolution from nonselective to active targeting system, Bioconjugate Chem. 26 (7) (2015) 1266–1276.
[28] M. Fotin-Mleczek, K.M. Duchardt, C. Lorenz, R. Pfeiffer, S. Ojkic-Zrna, J. Probst, et al., Messenger RNA-based vaccines with dual activity induce balanced TLR-7 dependent adaptive immune responses and provide antitumor activity, J. Immunother. 34 (1) (2011) 1–15.
[29] J. Banchereau, R.M. Steinman, Dendritic cells and the control of immunity, Nature 392 (6673) (1998) 245–252.
[30] M. Koivusalo, C. Welch, H. Hayashi, C.C. Scott, M. Kim, T. Alexander, et al., Amiloride inhibits macropinocytosis by lowering submembranous pH and preventing Rac1 and Cdc42 signaling, J. Cell Biol. 188 (4) (2010) 547–563. PMCID: 2828922.
[31] J. Kim, W.A. Li, Y. Choi, S.A. Lewin, C.S. Verbeke, G. Dranoff, et al., Injectable, spontaneously assembling, inorganic scaffolds modulate immune cells in vivo and increase vaccine efficacy, Nat. Biotechnol. 33 (1) (2015) 64–72.
[32] F.Y. Avci, X. Li, M. Tsuji, D.L. Kasper, A mechanism for glycoconjugate vaccine activation of the adaptive immune system and its implications for vaccine design, Nat. Med. 17 (12) (2011) 1602–1609.
[33] K.M. Uhlig, S. Schulke, V.A.M. Scheuplein, A.H. Malczyk, J. Reusch, S. Kugelmann, et al., Lentiviral protein transfer vectors are an efficient vaccine platform and induce a strong antigen-specific cytotoxic T cell response, J. Virol. 89 (17) (2015) 9044–9060.
[34] J.M. Trevejo, M.W. Marino, N. Philpott, R. Josien, E.C. Richards, K.B. Elkon, et al., TNF-alpha -dependent maturation of local dendritic cells is critical for activating the adaptive immune response to virus infection, Proc. Natl. Acad. Sci. U. S. A. 98 (21) (2001) 12162–12167. PMCID: 59785.
[35] C. Brunner, J. Seiderer, A. Schlamp, M. Bidlingmaier, A. Eigler, W. Haimerl, et al., Enhanced dendritic cell maturation by TNF-alpha or cytidine-phosphate-guanosine DNA drives T cell activation in vitro and therapeutic anti-tumor immune responses in vivo, J. Immunol. 165 (11) (2000) 6278–6286.
[36] C.D. Mills, K. Ley, M1 and M2 macrophages: the chicken and the egg of immunity, J. Innate Immun. 6 (6) (2014) 716–726. PMCID: 4429858.
[37] B.M. Carreno, M. Becker-Hapak, A. Huang, M. Chan, A. Alyasiry, W.R. Lie, et al., IL-12p70-producing patient DC vaccine elicits Tc1-polarized immunity, J. Clin. Invest. 123 (8) (2013) 3383–3394. PMCID: 3726168.

[38] B.M. Carreno, V. Magrini, M. Becker-Hapak, S. Kaabinejadian, J. Hundal, A.A. Petti, et al., Cancer immunotherapy. A dendritic cell vaccine increases the breadth and diversity of melanoma neoantigen-specific T cells, Science 348 (6236) (2015) 803–808. PMCID: 4549796.
[39] M. Fotin-Mleczek, K.M. Duchardt, C. Lorenz, R. Pfeiffer, S. Ojkic-Zrna, J. Probst, et al., Messenger RNA-based vaccines with dual activity induce balanced TLR-7 dependent adaptive immune responses and provide antitumor activity, J. Immunother. (Hagerstown, Md 1997) 34 (1) (2011) 1–15.
[40] E.S. Trombetta, I. Mellman, Cell biology of antigen processing in vitro and in vivo, Annu. Rev. Immunol. 23 (2005) 975–1028.
[41] T.N. Schumacher, R.D. Schreiber, Neoantigens in cancer immunotherapy, Science 348 (6230) (2015) 69–74.
[42] S.A. Shukla, M.S. Rooney, M. Rajasagi, G. Tiao, P.M. Dixon, M.S. Lawrence, et al., Comprehensive analysis of cancer-associated somatic mutations in class I HLA genes, Nat. Biotechnol. 33 (11) (2015) 1152–1158. PMCID: 4747795.
[43] M. Yadav, S. Jhunjhunwala, Q.T. Phung, P. Lupardus, J. Tanguay, S. Bumbaca, et al., Predicting immunogenic tumour mutations by combining mass spectrometry and exome sequencing, Nature 515 (7528) (2014) 572–576.